J|A|C|S
ARTICLES
Published on Web 06/28/2002

Investigations of Polyelectrolyte Adsorption at the Solid/Liquid Interface by Sum Frequency Spectroscopy: Evidence for Long-Range Macromolecular Alignment at Highly Charged Quartz/Water Interfaces

Joonyeong Kim, Gibum Kim, and Paul S. Cremer*

Contribution from the Department of Chemistry, Texas A&M University, P.O. Box 30012, College Station, Texas 77842-3012

Received March 24, 2002

Abstract: IR-visible sum frequency spectroscopy (SFS) was employed to investigate the molecular level details of the adsorption of the positively charged polyelectrolyte, polydiallyldimethylammonium chloride (PDDA), at the quartz/water interface. Below pH 9.0, signal from the interfacial water structure was visible, but none from the adsorbed polymer could be detected. This indicated that the PDDA was not well enough aligned at the interface under these conditions to elicit a sum frequency response. At more basic pH values ($\geq$9.6), however, adsorbed PDDA molecules became well-ordered as indicated by the presence of CH stretch peaks from methylene and methyl groups. The intensities of the CH stretch modes were independent of the adsorbed amount of PDDA at pH 12.3 but decreased as the pH of the bulk solution was lowered. The conditions for polymer alignment fell outside the parameters where layer-by-layer growth of oppositely charged polyelectrolytes was possible because the net charge on the surface under high pH conditions remained negative.

Introduction

Extensive investigations of monolayer and multilayer films have focused on the preparation of well-ordered structures. The goals of this research have ranged from building novel sensor devices to the creation of organically based nonlinear optical materials. Two major approaches for ordered film formation have included Langmuir−Blodgett (LB) and self-assembled monolayer (SAM) techniques.[1,2] Somewhat more recently, a new preparative method, layer-by-layer (LbL) deposition of polyelectrolytes from aqueous solution, has begun to gain notice. This relatively simple and effective procedure was developed by Decher and co-workers and is based upon the pioneering work of Iler et al.[3−5] The basic concept exploits the electrostatic attraction between a charged solid substrate and oppositely charged polyelectrolytes in solution. Positively and negatively charged polymers are sequentially introduced to a liquid/solid interface to create nanoscale supramolecular architectures. The methodology is quite flexible and has been employed in the formation of a variety of materials.[6−12]

Despite its rich potential for applications and relatively simple preparation requirements, investigators have only begun to explore the underlying mechanistic processes that govern multilayer formation from LbL deposition.[10,11,13,14] A molecular level understanding of such processes will be necessary if full exploitation of the LbL technique for highly tailored film geometries is to be achieved. Since LbL growth is mainly governed by electrostatic interactions, control over the surface charge density of the substrate is crucial for film construction. Adsorption under such highly charged conditions inevitably involves structural rearrangements of both the adsorbed polyelectrolytes and the associated interfacial water molecules.

As the interfacial regime usually exhibits spatial orientation with respect to an underlying charged substrate, infrared-visible sum frequency spectroscopy (SFS), a surface specific vibrational technique, and second harmonic generation (SHG) are ideal tools for investigation of these buried polymer interfaces.[15−24] In fact,

* To whom correspondence should be addressed. Telephone: 979-862-1200. Fax: 979-845-7561. E-mail: cremer@mail.chem.tamu.edu.

(1) Ulman, A. *An Introduction to Ultrathin Organic Films from Langmuir-Blodgett to Self-Assembly*; Academic Press: New York, 1991.
(2) Ulman, A. *Chem. Rev.* **1996**, *96*, 1533−1554.
(3) Iler, R. K. *J. Colloid Interface Sci.* **1966**, *21*, 569−594.
(4) Decher, G.; Hong, J. D.; Schmitt, J. *Thin Solid Films* **1992**, *210/211*, 831−835.
(5) Decher, G. *Science* **1997**, *277*, 1232−1237.
(6) Ferreira, M.; Rubner, M. F. *Macromolecules* **1995**, *28*, 7107−7114.
(7) Cheung, J. H.; Stockton, W. B.; Rubner, M. F. *Macromolecules* **1997**, *30*, 2712−2716.
(8) Mao, G.; Tsao, Y., −H.; Tirrell, M.; Davis, H. T. *Langmuir* **1995**, *11*, 942−945.
(9) van der Boom, M. E.; Richter, A. G.; Malinsky, J. E.; Lee, P. A.; Armstrong, N. R.; Dutta, P.; Marks, T. J. *Chem. Mater.* **2001**, *13*, 15−17.
(10) Dante, S.; Advincula, R.; Frank, C. W.; Stroeve, P. *Langmuir* **1999**, *15*, 193−201.
(11) Ariga, K.; Lvov, Y.; Kunitake, T. *J. Am. Chem. Soc.* **1997**, *119*, 2224−2231.
(12) Lvov, Y. M.; Lu, Z.; Schenkman, J. B.; Zu, X.; Rusling, J. F. *J. Am. Chem. Soc.* **1998**, *120*, 4073−4080.
(13) Sukhishvili, S. A.; Granick, S. *J. Am. Chem. Soc.* **2000**, *1222*, 9550−9551.
(14) Kurth, D. G.; Osterhout, R. *Langmuir* **1999**, *15*, 4842−4846.
(15) Kim, J.; Cremer, P. S. *J. Am. Chem. Soc.* **2000**, *122*, 12371−12372.
(16) Kim, J.; Cremer, P. S. *ChemPhysChem* **2001**, *2*, 543−546.
(17) Kim, J.; Kim, G.; Cremer, P. S. *Langmuir* **2001**, *17*, 7255−7260.
(18) Du, Q.; Freysz, E.; Shen, Y. R. *Phys. Rev. Lett.* **1994**, *72*, 238−241.
(19) Scatena, L. F.; Brown, M. G.; Richmond, G. L. *Science* **2001**, *292*, 908−912.
(20) Becraft, K. A.; Richmond, G. L. *Langmuir* **2001**, *17*, 7721−7724.

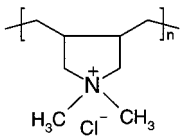

PDDA

Figure 1. Structure of PDDA.

SFS has already been used to obtain important information on the nature of noncrystalline polymer surfaces, which possess better molecular alignment than the corresponding bulk materials.[25,26] It has also been shown that changing the environment of the polymer surface from hydrophobic to hydrophilic can lead to changes in the alignment of interfacial pendant groups attached to the macromolecules.[27,28] We, therefore, reasoned that probing the interfacial polyelectrolyte and water structures via SFS might provide valuable information about the adsorption process as well as the ultimate polymer structure. It was felt that this could provide insight into the utility of the LbL method for creating nonlinear optical materials.

Recently, we reported that sequential deposition at the quartz/water interface of a positively charged polymer, PDDA, and a negatively charged polymer, the sodium salt of polystyrene sulfonic acid (PSS), dramatically affected the interfacial water structure.[15] In fact, SFS showed that interfacial water was best organized under acidic conditions if the final polymer layer was positively charged. By contrast, surface water molecules were found to be better organized under more basic conditions if the final layer was negatively charged. This was the case despite the fact that neither polymer was titratable under the condition employed in the experiment (pH 3.8 to 8.0).

In the present studies we deposited PDDA (Figure 1) onto bare quartz/water interfaces. The sum frequency (SF) spectra from these systems revealed the remarkable presence of CH stretch peaks under very basic conditions where the substrate charge density was quite high. The presence of ordered adsorbed polyelectrolyte molecules stood in stark contrast to lower pH conditions where no such alignment was observed. Significantly, the overall charge on the surface remained negative after polymer deposition from the highly basic solutions. This falls outside the parameters of LbL film growth conditions, which require net charge inversion upon the deposition of each successive polyelectrolyte layer. When the initial charge density is high enough, however, charge inversion does not take place, and LbL film growth becomes impossible.[29,30] We believe that the imposition of long-range order upon a charged macromolecule at an oppositely charged interface may be quite general under conditions where charge inversion does not occur. In this report results are presented for water structure and PDDA alignment as a function of pH, ionic strength, and adsorbed mass of polyelectrolyte.

Experimental Section

Laser System. Sum frequency spectra were obtained with a passive-active mode-locked Nd:YAG laser (PY61c, Continuum, Santa Clara, CA) equipped with a negative feedback loop in the oscillator cavity to provide enhanced shot-to-shot stability. The 1064 nm light generated had a pulse width of 21 ps, and the laser was operated at a 20 Hz repetition rate. Radiation was sent to an optical parametric generator/amplifier (OPG/OPA) stage (Laser Vision, Bellevue, WA) where tunable infrared radiation was produced in addition to frequency-doubled radiation at 532 nm. The OPG/OPA consisted of two parts. The first was an angle-tuned potassium titanyl phosphate (KTP) stage pumped with 532 nm light to generate near-infrared radiation between 1.35 and 1.85 μm. This output was then mixed with the 1064 nm fundamental in an angle-tunable potassium titanyl arsenate (KTA) stage to produce a tunable infrared beam from 2000 to 4000 cm^{-1} (7 cm^{-1} fwhm). The intensity of the radiation was approximately 500 μJ/pulse near 3500 cm^{-1}. The tunable IR beam was combined with the 532 nm radiation at the sample interface at incident angles of 51° and 42°, respectively, with respect to the surface normal. The power of the 532 nm beam, which was generated in an initial KTP stage, was 1 mJ/pulse at the sample. The sum frequency signal generated from the sample was collected by a photomultiplier tube, sent to a gated integrator, and stored digitally. For each scan, data were collected in 6 cm^{-1} increments in the 2800−3600 cm^{-1} range.

SFS. The theory and experimental setup of SFS have been described in detail elsewhere.[31,32] Briefly, sum frequency spectroscopy involves a second-order nonlinear optical process in which two input beams with frequencies ω_{ir} and ω_{vis} overlap in a medium to generate an output at the sum frequency, ω_{sf}. As a second-order process, SF signal is forbidden in the dipole approximation in media that possess inversion symmetry but allowed at surfaces and interfaces where inversion symmetry is necessarily broken. This technique, therefore, can be employed as an interface-specific probe for systems that possess bulk inversion symmetry. The intensity of the sum frequency signal, I_{sf}, is proportional to the square of the surface nonlinear susceptibility, $\chi^{(2)}$:

$$I_{sf} \approx |\chi^{(2)}|^2 I_{vis} I_{ir} = |\chi_{NR}{}^{(2)} + \sum \chi_{R\nu}{}^{(2)}|^2 I_{vis} I_{ir} \quad (1)$$

$$\chi_{R\nu}{}^{(2)} \approx A_\nu/(\omega_\nu - \omega_{ir} - i\Gamma_\nu) \quad (2)$$

where $\chi_{NR}{}^{(2)}$ and $\chi_{R\nu}{}^{(2)}$ denote the nonresonant and resonant contributions, respectively. The terms A_ν, ω_ν, and Γ_ν are the oscillator strength, resonant frequency, and damping constant of the νth resonant mode, respectively. All spectra presented in this work were collected with the s_{sf}, $s_{vis.}$, and p_{ir} polarization combination.

Materials. The water used in the preparation of sodium phosphate buffer solutions and in the cleaning of the experimental apparatus was purified with a NANOpure Ultrapure Water System (Barnstead, Dubuque, IA) with a minimum resistivity of 18 MΩ·cm. PDDA (MW 400000−500000, Aldrich), was used to prepare 1.0 mg/mL stock solutions adjusted to pH 1.5, 3.8, 5.6, 8.0, 9.6, and 12.3 (sodium phosphate/phosphoric acid for pH 3.8, 5.6, 8.0, and 9.6; 0.5 M HCl for pH 1.5; 0.5 M NaOH for pH 12.3). Appropriate amounts of analytical reagent grade NaCl were added to increase the total electrolyte concentration to the desired value. Polyelectrolyte free buffer solutions were also used in these studies and prepared in the same manner as above, but without PDDA. Control experiments were performed at all pH values both with and without phosphate buffer. The presence of the buffer in solution had no noticeable affect on the SF spectra obtained within experimental error. Infrared-grade fused quartz windows

(21) Gragson, D. E.; Richmond, G. L. *J. Am. Chem. Soc.* **1998**, *120*, 366−375.
(22) Baldelli, S.; Schnitzer, C.; Shultz, M. J. *J. Phys. Chem. B.* **1997**, *101*, 4607−4612.
(23) McAloney, R. A.; Goh, M. C. *J. Phys. Chem. B* **1999**, *103*, 10729−10732.
(24) Zhao, X.; Ong, S.; Eisenthal, K. B. *Chem. Phys. Lett.* **1993**, *202*, 513−520.
(25) Chen, Z.; Ward, R.; Tian, Y.; Baldelli, S.; Opdahl, A.; Shen, Y. R.; Somorjai, G. A. *J. Am. Chem. Soc.* **2000**, *122*, 10615−10620.
(26) Gracias, D. H.; Chen, Z.; Shen, Y. R.; Somorjai, G. A. *Acc. Chem. Res.* **1999**, *32*, 930−940.
(27) Chen, Q.; Zhang, D.; Somorjai, G.; Bertozzi, C. R. *J. Am. Chem. Soc.* **1999**, *121*, 446−447.
(28) Wang, J.; Woodcock, S. E.; Buck, S. M.; Chen, C.; Chen, Z. *J. Am. Chem. Soc.* **2001**, *123*, 9470−9471.
(29) Joanny, J.-F. *Eur. Phys. J. B* **1999**, *9*, 117−122.
(30) Netz, R. R.; Joanny, J.-F. *Macromolecules* **1999**, *32*, 9013−9025.
(31) Shen, Y. R. *Nature* **1989**, *337*, 519−525.
(32) Shen, Y. R. *Surf. Sci.* **1994**, *299/300*, 551−562.

(o.d. 1 in., thickness $^1/_{16}$ in.) were purchased from Quartz Plus Inc. (Brookline, NH). They were prepared by cleaning in hot chromic acid for several hours, rinsing with copious quantities of purified water, and baking in a kiln at 400 °C overnight before use.

Data Collection and Controls. Experimental measurements were carried out using a homemade flow-cell (volume ca. 2.0 mL) which consisted of a machined Teflon body fitted with a fused quartz plate. The incoming laser beams were focused concentrically on the bottom face of the fitted quartz plate where polymer adsorption occurred. The sides of the cell included an inlet and an outlet port to which Tygon tubing (i.d. 0.06 in.) was attached for flowing polyelectrolyte solutions. Polymer deposition was initiated by flowing PDDA solution (20 mL) over the bare quartz/water interface for 200 s followed by removing excess PDDA using sufficient amounts of buffer solution (100 mL) with the same pH and total electrolyte concentration. To change the pH of the bulk solution in the flow cell, stock solution at the desired pH value was allowed to flow until the value at the outlet port varied by less than ±0.1 pH units compared with that at the inlet port.

Results

a. pH Effect. Since fused quartz surfaces are terminated by titratable silanol groups, raising the pH causes an increase in the interfacial charge density at the aqueous interface.[33] Below pH 3 nearly all the surface silanols are protonated, and the surface charge becomes neutralized. On the other hand, at pH 12.3 nearly all surface silanols are deprotonated, leaving the surface with a very high net negative charge. The increase in charge density at higher pH leads to a larger electric field, which aligns more water molecules near the interface than under acidic conditions. This alignment manifests itself as a general increase in SF signal in the OH stretch range as the pH is increased above the bare quartz/water interface from pH 3.8 to 12.3 (Figure 2a). A slight rise in signal is also noted as the pH is decreased from pH 3.8 to 1.5 (Figure 2a). This has been previously attributed to hydrogen bonding between oxygen atoms in interfacial water molecules with the surface silanol moieties.[18] Another possibility is that the surface may become slightly positively charged under very acidic conditions, which would also lead to increased alignment. The SF data demonstrating these phenomena are in good agreement with previous investigations.[15,18,24] Two major spectroscopic features are noted at all pH values. A low-frequency peak is seen near 3200 cm^{-1}, which can be assigned to the OH symmetric stretch of tetrahedrally coordinated water molecules or "ice-like" molecular structure.[18,34,35] The second peak around 3400 cm^{-1} is from water molecules with less ordered hydrogen bonding or "water-like" structure.[18,34]

Figure 2b shows SF spectra of the quartz/water interface under the same buffer conditions after adsorption of PDDA from bulk solution. As can be clearly seen from the data, the trend from pH 1.5 to 9.6 is nearly the reverse of that seen from bare quartz. Namely, the ice-like peak intensity is strongest at pH 1.5 and weakest at pH 9.6. The reason for this stems from the inversion of the ζ-potential[36] at the interface upon polyelectrolyte adsorption.[15] The highest positive charge is achieved under conditions

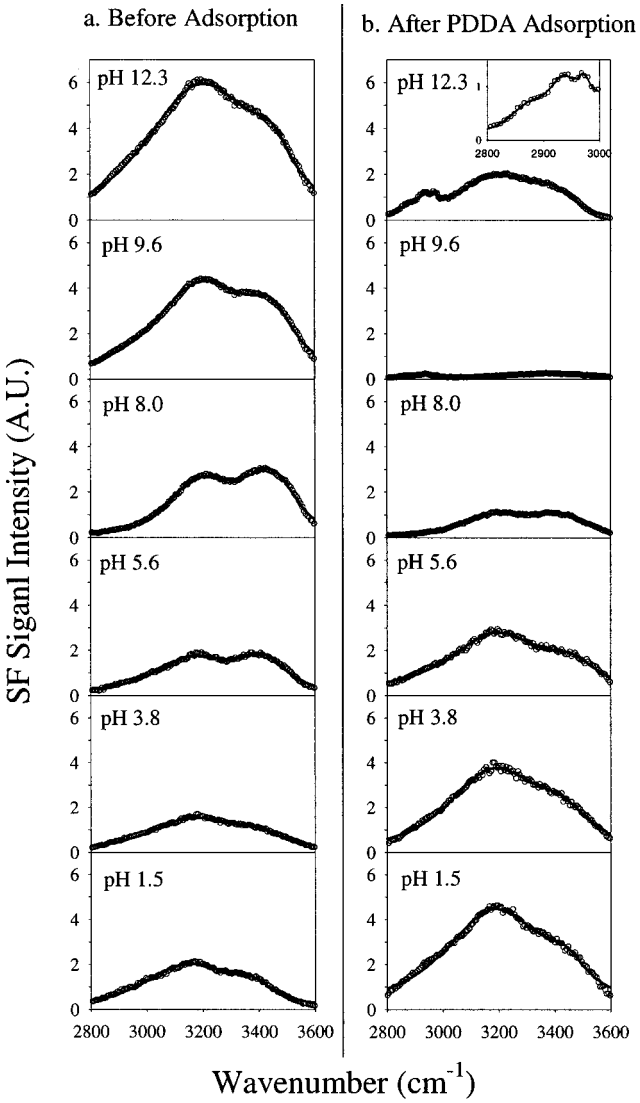

Figure 2. SFS spectra of the quartz/water interface in the OH stretch region between pH 1.5 and 12.3 (a) before and (b) after adsorption of PDDA. The solid lines are calculated fits to the data using a Voigt function from which peak positions, widths, and oscillator strengths can be obtained. The inset shows an enlargement of the CH stretch region. The beam polarizations employed were s (sum frequency), s (visible), and p (infrared).

where the original negative surface charge was smallest. Such an inversion of charge is crucial to the formation of multilayer thin films via the layer-by-layer growth technique of alternating deposition of negatively and positively charged polyelectrolytes.[5,15,29,30,37,38]

With continued increase in the pH, the amount of deposited PDDA continued to increase;[39,40] however, the adsorption became insufficient to reverse the sign of the interfacial charge, and the interface remained negatively charged. Theoretical modeling of such conditions indicated that charge inversion is prevented when the screening length of the charge is quite short and the total amount of positively charged polymer adsorbed is

(33) Iler, R. K. *The Chemistry of Silica*; Wiley: New York, 1979.
(34) Eisenberg, D.; Kauzmann, W. *The Structure and Properties of Water*; Oxford University Press: New York, 1969.
(35) Walrafen, G. E. In *Raman and Infrared Spectral Investigations of Water Structure*; Franks, F., Ed.; Plenum: New York, 1972; Vol. 1, pp 151−214.
(36) ζ-Potential is defined as the potential difference between the bulk liquid and the shear plane in the electric double layer where ions begin to move.
(37) Ladam, G.; Schaad, P.; Voegel, J. C.; Schaaf, P.; Decher, G.; Cuisinier, F. *Langmuir* **2000**, *16*, 1249−1255.
(38) Caruso, F.; Donath, E.; Möhwald, H. *J. Phys. Chem. B* **1998**, *102*, 2011−2016.
(39) Schwarz, S.; Buchhammer, H.-M.; Lunkwitz, K.; Jacobasch, H.-J. *Colloid Surf., A* **1998**, *140*, 377−384.
(40) Bauer, D.; Buchammer, H.; Fuchs, A.; Jaeger, W.; Killmann, E.; Lunkwitz, K.; Rehmet, R.; Schwarz, S. *Colloid Surf. A* **1999**, *156*, 291−305.

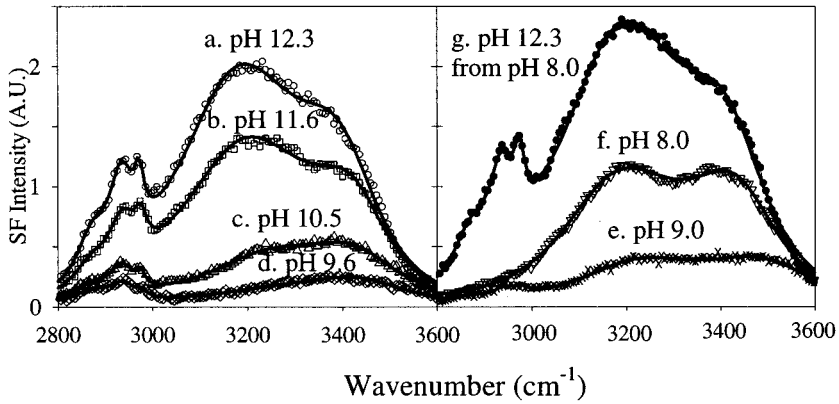

Figure 3. SFS spectra in the OH and CH stretch regions of the quartz/PDDA/water system at (a) pH 12.3 (○), (b) pH 11.6 (□), (c) pH 10.5 (△), (d) pH 9.6 (◇), (e) pH 9.0 (×), (f) pH 8.0 (▽), and (g) pH 12.3 followed by pH 8.0 (●). The solid lines are fits to the data. The data are split between two diagrams to avoid spectral crowding.

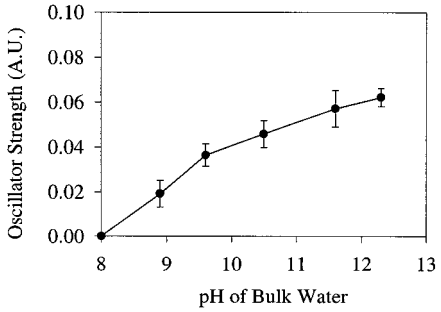

Figure 4. Fitted oscillator strengths from the CH stretch mode at 2935 cm^{-1} as a function of bulk pH shown in Figure 3.

high.[29,30] This was the case at pH 12.3 where the SF signal in the OH stretch range from the water/PDDA/quartz system was higher than after deposition at pH 9.6, although it was significantly lower than from the bare quartz surface at pH 12.3 (Figure 2). More significantly, new features began to arise in the CH stretch range that were not seen under lower pH conditions where the sign of the ζ-potential did invert upon polymer deposition. The CH stretch peaks can be assigned to CH_2 and CH_3 moieties of the macromolecule.[25,41,42] At least three individual modes at 2865, 2935, and 2970 cm^{-1} were present. It should be emphasized that in the dipole approximation SFS only generates signal from systems where centrosymmetry is broken. Because of this selection rule, the presence of these CH stretch features demonstrated that the polymer took on an ordered arrangement with respect to the interface at pH 12.3.

To further investigate the effect of bulk pH on the ordering of adsorbed PDDA, pH cycling experiments were performed after initial adsorption at pH 12.3. Figure 3, a−f, show spectra from the quartz/PDDA/water interface upon decreasing the pH in the presence of a PDDA film adsorbed at pH 12.3. Figure 3g shows the same system after cycling back to pH 12.3. For quantitative analysis of Figure 3, a−f, the values of the oscillator strengths (A_ν in eq 2) from the CH stretch feature at 2935 cm^{-1} were plotted as a function of pH, and the results are shown in Figure 4. These data show that the intensities of the CH stretch modes gradually decreased as the pH was lowered from 12.3 and disappeared by pH 8.0. On the other hand, the strength of the ice-like peak near 3200 cm^{-1} decreased only until pH 9.6 where it reached a minimum. Lowering the pH to 8.0 allowed the interface to invert the sign of the ζ-potential.[29,30,39,40] At this point the ice-like peak began increasing again, and all evidence for the CH stretch modes disappeared (f in Figure 3). Reverting back to pH 12.3 revealed the return of the CH stretch features (g in Figure 3). Moreover, the system could be cycled many times and both the CH and OH stretch features seemed to be reversible with the exception of a small increase in the OH spectral intensities (approximately 10%) that occurred after the first cycle. This increase probably corresponded to a small amount of PDDA desorption upon initially lowering the bulk pH. Also, the tiny residual CH stretch intensity which remained upon lowering the bulk pH to 9.0 (Figure 3e) was probably indicative of a certain amount of hysteresis in the system.

b. Effect of Adsorbed PDDA Amount. Experiments were performed at pH 12.3 as a function of the adsorbed amount of PDDA to determine whether the SF signal from the CH stretch modes emanated from the entire polymer layer or just the portion closest to the quartz interface. To vary the adsorption quantity, deposition was carried out at several pH values (12.3, 9.6, 8.0, 5.6, 3.8, and 1.5) followed by raising the pH to 12.3. It is known that the total mass of PDDA deposited is increased by over an order of magnitude (from approximately 0.02 mg/m^2 at pH 4 to over 0.7 mg/m^2 near pH 11) as the pH above the quartz/water interface is increased.[39,40] The system was extensively flushed with buffer (~50x the flow cell's volume) at the adsorption pH to remove all excess PDDA from the bulk solution before the pH was raised. Figure 5 shows the SF spectra from the quartz/PDDA/water systems at pH 12.3 for all six deposition conditions investigated. Curve-fitting the data revealed relatively little variation in the signal intensity of the CH stretch modes as a function of the adsorption conditions. The results for the peak at 2935 cm^{-1} are shown in Figure 6. It thus seems reasonable to postulate that only the PDDA closest to the interface was actually well enough aligned to participate in the creation of sum frequency signal as the experiment was insensitive to the amount of adsorption.

In contrast to the constancy of the oscillator strength of the CH stretch modes, the strength of the ice-like peak near 3200 cm^{-1} was strongest when PDDA adsorption was performed at pH 1.5 and weakest at pH 12.3 (Figure 5). The reason stems from the fact that reduced deposition of the positively charged PDDA corresponded to diminished ability to attenuate the

(41) Gragson, D. E.; Richmond, G. L. *J. Phys. Chem. B* **1998**, *102*, 3847−3861.
(42) Richmond, G. L. *Anal. Chem.* **1997**, *17*, 5536A-543A.

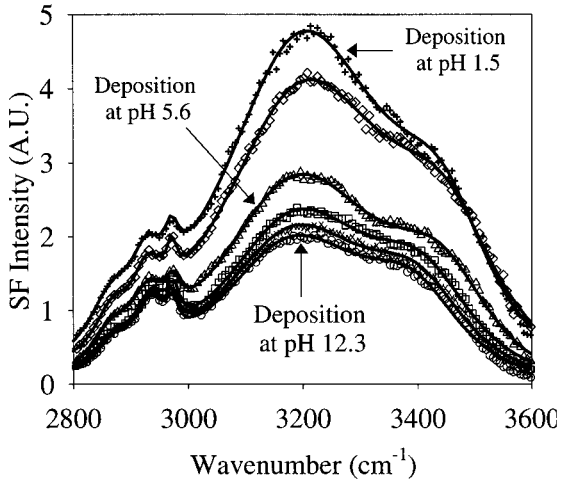

Figure 5. SFS spectra of the quartz/PDDA/water system at pH 12.3 in the OH and CH stretch regions after deposition at pH 12.3 (○), pH 9.6 (×), 8.0 (□), 5.6 (△), 3.8 (◇), and 1.5 (+). The pH of all systems was adjusted to 12.3 before the spectra were obtained. The solid lines are fits to the data.

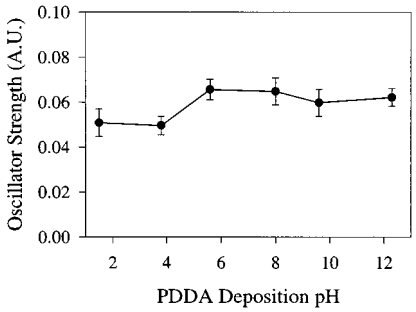

Figure 6. Fitted oscillator strengths from the CH stretch mode at 2935 cm^{-1} as a function of deposition pH shown in Figure 5.

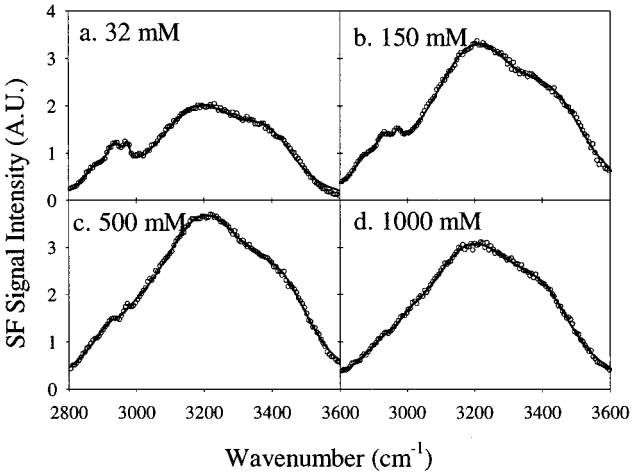

Figure 7. SFS spectra in the OH and CH stretch region from the quartz/PDDA/water interface at pH 12.3 and various values of total electrolyte concentration: (a) 32 mM, (b) 150 mM, (c) 500 mM, and (d) 1000 mM.

surface potential (and hence the ice-like peak strength) at the net negatively charged interface.

c. Effect of Electrolyte Concentration. Figure 7 shows SF spectra of the quartz/PDDA/water interface at pH 12.3 at different total electrolyte concentrations (32, 150, 500, and 1000 mM). By raising the total electrolyte concentration, peaks due to the CH stretch modes were attenuated and disappeared when the total concentration reached 1000 mM. On the other hand, the ice-like peak intensity at first increased (32 to 500 mM), but finally decreased as the total electrolyte concentration was raised to 1000 mM.

It has been shown in previous studies that the amount of adsorbed PDDA decreased at a given pH as the electrolyte concentration was increased.[43,44] The decrease in CH intensities, however, cannot be explained simply in terms of a decrease in the interfacial PDDA concentration as demonstrated by the results of Figures 5 and 6. Rather, the decreased intensity was likely caused by enhanced charge screening as the electrolyte concentration was raised.

The OH stretch results were more curious and probably the result of two competing phenomena. First, as the ionic strength was increased, the amount of PDDA on the surface was attenuated as mentioned above. This should have led to increased OH stretch signal as the net negative charge at the interface was increased. On the other hand, increasing the ionic strength also increased charge screening. This in turn caused the water layer at the interface to become more disordered. It appears that the charging effect was dominant until about 500 mM, at which point the amount of adsorbed PDDA was quite small, and hence, the primary effect of further increasing the ionic strength was to screen the interfacial charge and in turn disorder the interfacial water.

Discussion

We have explored the behavior of PDDA at the quartz/water interface as a function of pH and ionic strength. A central question that needs to be addressed in these experiments pertains to the exact source of the sum frequency signal from the polyelectrolyte layer. Potential candidates include the polymer material directly adjacent to the quartz substrate, the material at the polymer/buffer interface, or even the middle of the polymer layer. The results from Figures 2−4 demonstrate that uniquely under high pH conditions the PDDA molecules became well-aligned at the interface. This behavior was fairly reversible (Figure 3) and appears to argue for at least some of the signal originating from the polymer material closest to the surface where the PDDA can most strongly interact with the deprotonated surface silanols. One may consider a molecular level picture for the increase in ordering of polymer material adjacent to the quartz surface as the bulk pH is raised. Both experimental and theoretical studies have revealed that increasing the surface charge density induces more compact packing of electrostatically adsorbed polyelectrolytes. The process works by transforming the loosely packed globular coil conformation into a more compact layer with a net decrease in layer thickness.[44−46]

Since the surface charge density affected the extent of interfacial polymer alignment near the substrate surface, it would be reasonable to assume that raising the solution's ionic strength should attenuate the CH stretch signal by decreasing the screening length (Figure 7). When the adsorption of polyelectrolytes onto the charged quartz surface was carried out at low electrolyte concentration, polyelectrolytes needed to adopt flatter conformations, owing to electrostatic repulsion between the

(43) Ostrander, J. W.; Mamedov, A. A.; Kotov, N. A. *J. Am. Chem. Soc.* **2001**, *123*, 1101−1110.
(44) Shubin, V.; Linse, P. *Macromolecules* **1997**, *30*, 5944−5952.
(45) Dobrynin, A. V.; Deshkovski, A.; Rubinstein, M. *Phys. Rev. Lett.* **2000**, *84*, 3101−3104.
(46) Borisov, O. V.; Zhulina, E. B.; Birshtein, T. M. *J. Phys. II* **1994**, *4*, 913−929.

charged polymer chains.[47−49] At higher electrolyte concentration, however, the repulsion between the PDDA molecules can be reduced due to charge screening, and the adsorbed polyelectrolytes are allowed to adopt more "loopy" structures with increased thickness at a given pH as suggested by previous studies.[7,47−50] These latter structures are almost certainly less well-ordered and, hence, gave rise to the decrease in sum frequency signal in the CH stretch range as the ionic strength was increased.

The data in Figures 5 and 6 indicate that the CH stretch signal is essentially independent of layer thickness. This appears to rule out the possibility that signal is emanating from the middle of the polymer layer. The experiments from Figures 2−7, however, do not completely rule out the possibility that some portion of the signal emanates from the polymer/buffer interface. Nevertheless, this possibility seems unlikely. The material at the polymer/buffer interface is screened from the fixed substrate charge by the intervening polymer strands. Furthermore, it would be quite difficult to explain the strong pH dependence of the CH stretch signal if it were to arise from the polymer/buffer interface since the polymer itself contains no titratable groups.

The behavior of the quartz/PDDA/water system may prove to be quite general as we have recently observed similar results for lysozyme (pI = 11.0) adsorbed at the quartz/water interface. In that case, CH stretch modes were also uniquely present at high pH values where the surface rather than the positively charged biomacromolecules determined the sign of the ζ-potential.[51] A picture seems to be emerging of distinct behavioral regimes for adsorbed macromolecules on oppositely charged substrates. When the substrate charge density is low or the ionic strength of the solution is sufficiently high, the repulsions between the charged pendant groups on the macromolecules lead to a largely disordered structure at the interface. On the other hand, charged pendant groups in close proximity to the interface become aligned with respect to the surface normal when the ionic strength of the bulk solution is low and the initial charge density of the substrate is sufficiently high to prevent inversion of the ζ-potential upon adsorption (Figure 8).

The above findings are significant in light of the numerous second-harmonic generation studies that have been performed in search of thin films that retain inversion symmetry during the layer-by-layer growth process.[23,52,53] Indeed, the present studies show the difficulty in using electrostatic forces alone to align organic layers for use as nonlinear optical materials. This is because the conditions that allow for the establishment of well-ordered films are exactly those that do not allow LbL growth to take place. It therefore seems apparent that other forces such as steric or hydrogen bonding in more rigid molecular architectures are required to align the dipoles in each layer. Examples of such strategies include organic−inorganic hybrid nanocomposites,[54] asymmetric metal−organic complexation,[55] hydrophobic interactions between substrates and chromophores,[53] and covalent attachment of multilayers.[56] Since these chemistries require greater sophistication than simple adsorption, it is still unknown whether Langmuir−Blodgett methods or the LbL strategy will ultimately provide the superior route to growing nonlinear optical films.

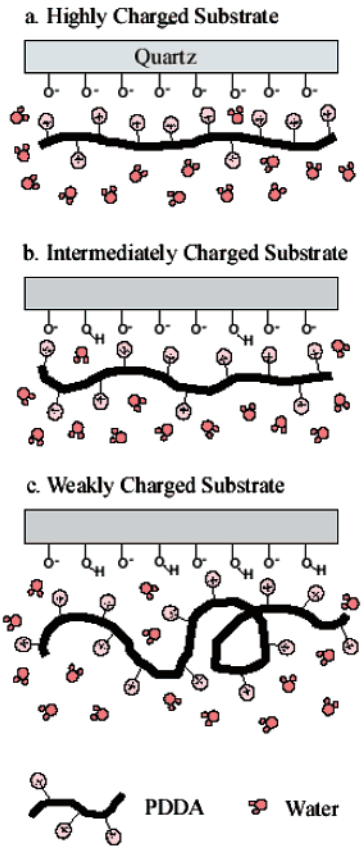

Figure 8. Schematic representation of adsorbed PDDA at the quartz/water interface from (a) a highly charged substrate, (b) an intermediately charged substrate, and (c) a weakly charged substrate.

Conclusions

We monitored the deposition of PDDA, a positively charged polyelectrolyte, at the quartz/water interface by SFS. CH stretch modes were observed at high pH (≥9.6), and their intensities were attenuated upon lowering the pH. The strengths of these peaks were dependent upon total electrolyte concentration but were nearly independent of the amount of PDDA adsorbed. Unlike lower pH conditions, the surface charge was not inverted by PDDA adsorption at pH 12.3.

Acknowledgment. This research was generously supported by the National Science Foundation (CHE-0094332), the Robert A. Welch Foundation (Grant A-1421), and a Research Innovation Award from the Research Corporation (Grant RI0437).

Supporting Information Available: Tables S1 and S2 of curve-fit results for Figures 2, 3, and 5 (PDF). This material is available free of charge via the Internet at http://pubs.acs.org.

JA0263036

(47) Dubas, S. T.; Schlenoff, J. B. *Macromolecules* **1999**, *32*, 8153−8160.
(48) Dubas, S. T.; Schlenoff, J. B. *Langmuir* **1999**, *17*, 7725−7727.
(49) McAloney, R. A.; Sunyor, M.; Dudnik, V.; Goh, M. C. *Langmuir* **2001**, *17*, 6655−6663.
(50) Decher, G.; Schmitt, J. *Prog. Colloid Polym. Sci.* **1992**, *89*, 160−164.
(51) Kim, G.; Gurau, M.; Kim, J.; Cremer, P. S. *Langmuir* **2002**, *18*, 2807−2811.
(52) Lee, S. H.; Balasubramanian, S.; Kim, D. Y.; Viswanathan, N. K.; Bian, S.; Kuman, J.; Tripathy, S. K. *Macromolecules* **2000**, *33*, 6534−6540.
(53) Roberts, M. J.; Lindsay, G. A.; Herman, W. N.; Wynne, K. J. *J. Am. Chem. Soc.* **1998**, *120*, 11202−11203.
(54) Kim, D. W.; Blumstein, A.; Kumar, H.; Tripathy, S. K. *Chem. Mater.* **2001**, *13*, 243−246.
(55) Bakiamoh, S. B.; Blanchard, G. J. *Langmuir* **2001**, *17*, 3438−3446.
(56) Sun, J.; Wu, T.; Lui, F.; Wang, Z.; Zhang, X.; Shen, J. *Langmuir* **2000**, *16*, 4620−4624.